Evaluations of coating high-speed runnability using pilot coater data, rheological measurements, and computer modeling

John A. Roper III and Jamel F. Attal

ABSTRACT: Coating rheology data were collected using rotational viscometers for low-shear measurements and a capillary viscometer for high-shear measurements. The viscosity data were combined to generate a single flow curve for each formulation covering shear rates from 1 s^{-1} to 1,000,000 s^{-1}. This flow curve was fitted with a five-parameter model using an extension of the Cross equation to include dilatancy at high shear rates. This rheology model was incorporated into a computational fluid dynamics (CFD) simulation of a short-dwell coater which took into consideration differences in coater geometry. The blade pressures calculated from the computer model were compared with pilot coater data for the same formulation.

KEYWORDS: Coaters, computers, high velocity, measurement, models, rheological properties, runnability.

Paper coating is an important industrial process used to improve the appearance and printability of paper. A variety of coater configurations are used to apply paper coatings—roll applicator, short dwell, and rod coaters. In this paper, the discussion will be limited to short-dwell coaters which are used to apply lightweight coatings (4–6lb/3300 ft^2) at high coating speeds. The purpose of this study was to improve the high-speed runnability of coating formulations used in lightweight coated (LWC) papers. In order to do this, however, we first had to develop ways to evaluate the high-speed runnability of paper coatings.

For our purposes, high speed is defined as 3500 ft/min or greater. Good runnability is defined as having a clean blade with good coat weight control without using high blade pressures. In recent years as coating speeds have increased beyond 3500 ft/min, several runnability problems have occurred. These include visual defects such as buildup of coating on the blade, spraying-misting-spitting of the coating, and scratching of the coating. Another type of problem concerns coat weight control such as poor coating profile uniformity across the paper or excessively high blade pressures needed to achieve the desired coat weights. High blade pressures lead to an increased frequency of web breaks and downtime on the paper machine.

One of the difficulties in addressing runnability problems is that there are several underlying causes with more than one solution. It is well known that runnability depends on coater geometry, basestock properties, and the coating formulation *(1–5)*. Because of the complex interrelationship between the factors controlling high-speed runnability, it is not possible to predict high-speed runnability simply from laboratory rheological measurements. Generally, high-speed runnability is evaluated using a pilot coating facility which more closely simulates the actual coating conditions in a paper mill. At the pilot coater, one can test a formulation on the basestock of interest at a speed matching that of the actual paper coating machine. This approach is time consuming, expensive, and requires large volumes of materials. Ideally, one would like a way to predict high-speed runnability from simple measurements in the laboratory in order to screen formulations at an early stage of development.

Our approach to this problem has been to combine laboratory rheologi-

Roper is research leader and Attal is research engineer with Dow Chemical Co., Midland, MI 48674.

cal measurements with computer modeling. The objective is to use computational fluid dynamics (CFD) as a tool for predicting and understanding high-speed runnability along with actual pilot coater experience. At this time, we have incorporated the coating rheology profile and different coating head designs into the model. As we continue to develop the CFD model, we hope to minimize the need for pilot coater testing.

Our work can be divided into four parts. The first part is the evaluation at the Dow pilot coater of high-speed runnability of LWC coating formulations. The second part is the rheological characterization of these formulations over a wide shear rate range. The third part is the development of a rheology model to fit the viscosity versus shear rate data of our coating formulations. The fourth part is the development of the CFD model to simulate the coating process. Each of these parts will be discussed in turn.

Pilot coater studies

The pilot coater is a useful tool for evaluating high-speed runnability of paper coatings. However, it is important to recognize that there are limitations which must be considered when using the pilot coater. One limitation is the short running time (10–12 min), which does not allow the system to reach equilibrium conditions. This makes it crucial to set the head angle to the proper setting to ensure that the blade face is running parallel to the paper web at the onset of the test. Also, the blade experiences more times of acceleration and deceleration at the pilot coater than in a mill. We found that the majority of the blade wear occurred during these changes in speed. Buildup of coating behind the blade was also affected by the acceleration and deceleration stages of the experiment, and this could lead to erroneous conclusions. We developed test conditions to control both the blade nip geometry and blade wear to give more reproducible results. The reasons for this are given in the next section.

Evaluating runnability

Based on our experience at the pilot coater, we have identified at least three distinct types of runnability problems which can occur concurrently or separately from each other. The first type of runnability problem appears as "visual defects"—weeping, whiskering, spitting, or spraying at the blade. We found that a key parameter for this kind of runnability problem is the angle of the blade face with the paper, as shown in **Fig. 1**. Runnning on the land of the blade is the optimum condition and usually results in a clean blade, although weeping is observed for systems with poor high-shear rheology. Running on the heel of the blade causes problems such as weeping, spraying, and misting even for formulations with good high-shear rheology. Running on the toe causes dry whiskering on the blade and increased web breaks. Because the blade is flexible, the actual blade tip angle depends on the initial blade angle, blade thickness, coating speed, and coating rheology. Thus, when evaluating a formulation's impact on blade weeping or whiskering, it was necessary to choose the proper blade thickness and head angle for a given coating speed and/or coating rheology to ensure running on the land of the blade. This allowed valid comparisons to be made between formulations and eliminated the interference of blade nip geometry on the results.

A second type of runnability problem is related to colloidal and shear instabilities in the coating. These problems show up as excessive buildup of coating behind the blade, scratching, or drift in coat weight over time. Often there is a long induction time before these problems occur. This makes it difficult to test for these problems on the pilot coater because the running times are short. Also, this type of problem seems more prevalent with higher solids coatings and when using a roll-applicator rather than a short-dwell coater. This type of runnability problem is not as dependent on coating speed as are other runnability problems.

1. Definitions of blade nip geometry

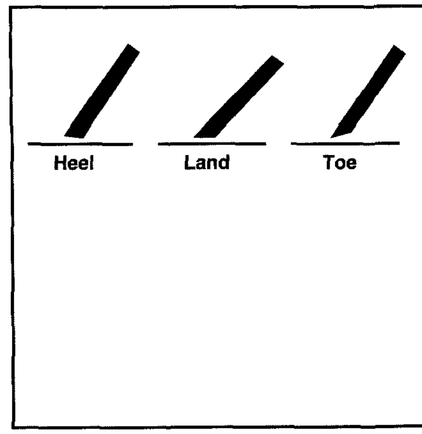

2. Method for comparing runnability of coating formulations

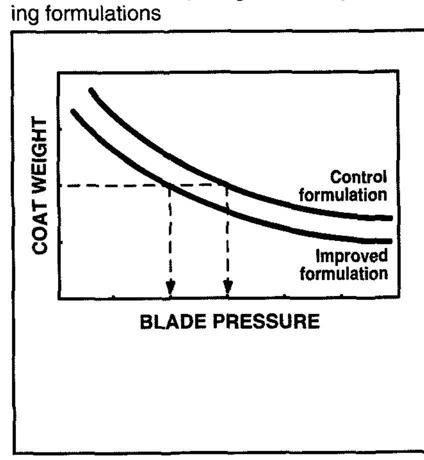

The third type of runnability problem concerns coat weight control—either obtaining nonuniform coat weights across the web or using high blade pressures to achieve the target coat weight. For lightweight coating applications, it is desirable to minimize the blade pressure needed to reach a target coat weight to avoid web breaks. To test for this property one can measure the coat weight response of a coating formulation as a function of blade pressure, as shown in **Fig. 2**.

Conceptually, this approach is simple. In practice, however, it proved difficult to get reproducible results. We found that the blade pressure needed to reach a target coat weight could vary by over 50% for the same formulation. One major reason for this is wear of the blade. As the blade pressure was varied during the run to give

3. Correlation of high-shear capillary viscosity at 1,000,000 s-1 with blade pressure needed to achieve 5.5-lb coat weight at 3500 ft/min

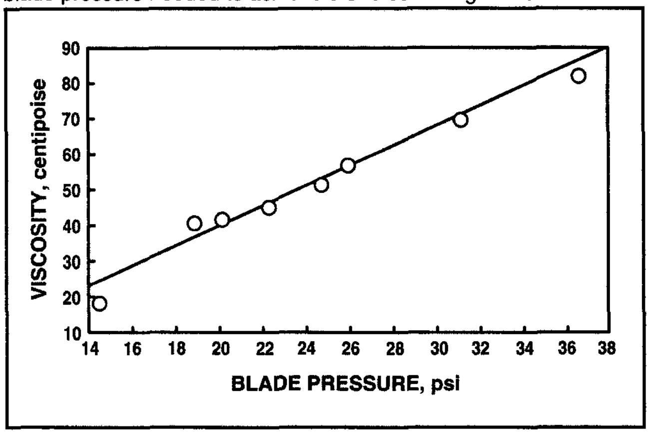

4. Correlation of high-shear capillary viscosity at 1,000,000 s-1 with blade pressure at 3500 ft/min when running on toe of blade

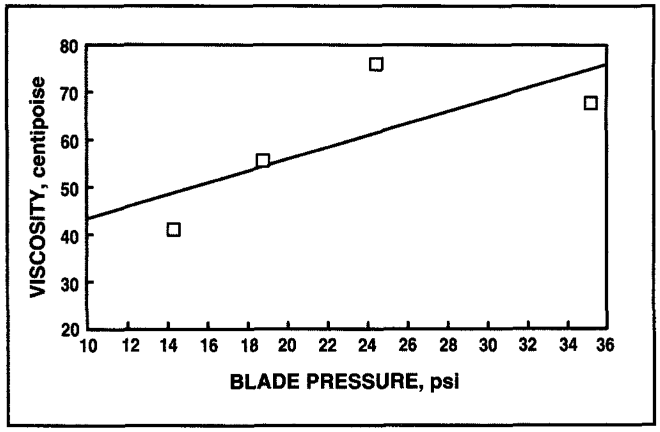

5. Combined viscosity versus shear rate data for control formulation

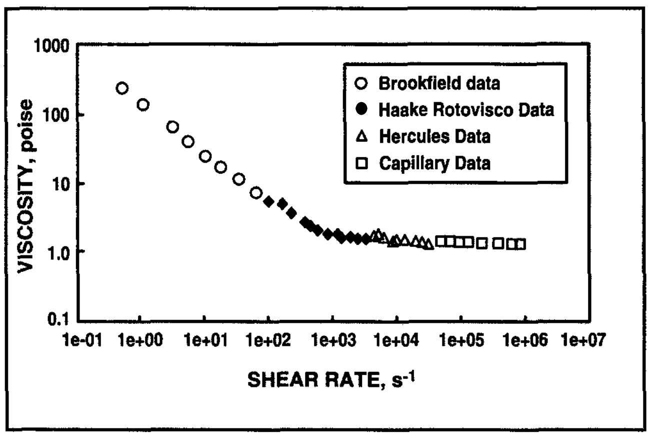

6. Typical viscosity versus shear rate data for starch-containing formulations at 62% solids

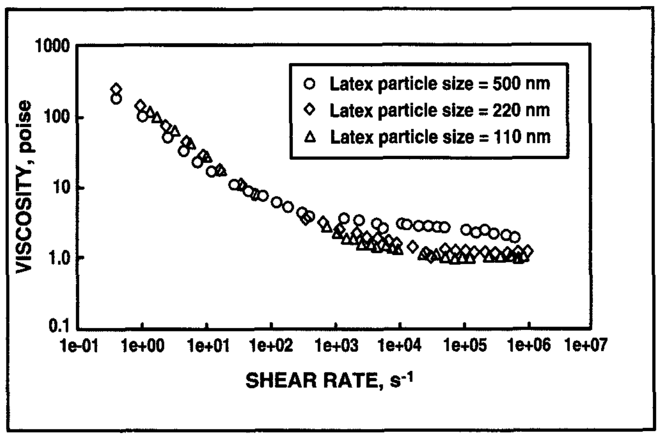

different coat weights, this would round off the blade face and change the effective area through which the blade pressure is transmitted. We switched to ceramic coated blades, which are much more durable, to minimize blade wear as a factor. Once we controlled both the blade nip geometry and the degree of blade wear, we were able to get consistent and reproducible results for the coat weight response.

Correlation of runnability with rheology

Coating rheology plays an important role in the performance of a coating formulation. Under the blade, shear rates exceed 1,000,000 s^{-1}, so good high-shear behavior of the coating is needed for high-speed runnability. **Figure 3** shows a plot of the blade pressure needed to reach 5.5 lb/3300 ft^2 coat weight versus the viscosity at 1,000,000 s^{-1} for a series of formulations tested at the Dow high-speed pilot coater. These formulations contained 75 parts delaminated clay, 25 parts No. 2 clay, 8 parts starch, and 8 parts latex. The type of starch and latex was varied as well as the coating solids level. The formulations were coated onto a 28 lb basestock containing groundwood. These data were collected using coater conditions to run on the land of the blade and minimize blade wear, as described above. For this set of formulations there was an excellent correlation between the high-shear viscosity and the blade pressure. In general, we confirmed that coating rheology is an important factor for runnability problems with coat weight control. However, for problems such as blade weeping and spitting, the coater configuration is more important than high-shear rheology. This supports the ideas in Gane's paper *(6)* in which he states that blade nip geometry is a key factor for stalagmite formation.

Figure 4 shows a plot of high-shear viscosity versus blade pressure for a set of formulations which were coated while running on the toe of the blade. Under these coating conditions, there was a poor correlation of high-shear viscosity with runnability. In fact, we found that the water holding property of the formulation was more important than the high-shear viscosity in determining runnability under these conditions. This illustrates that high-speed runnability is a complex phenomenon in which coating rheology is only one of the contributing factors. This was our reason for using com-

7. Combined viscosity versus shear rate data for dilatant formulation

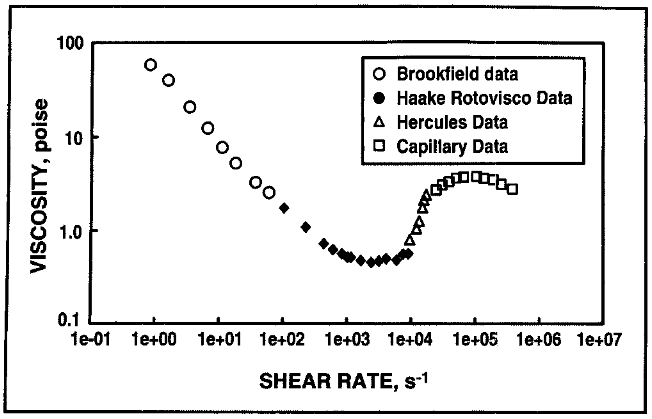

8. Effect of latex particle size on viscosity versus shear rate data for formulation solids level of 64%

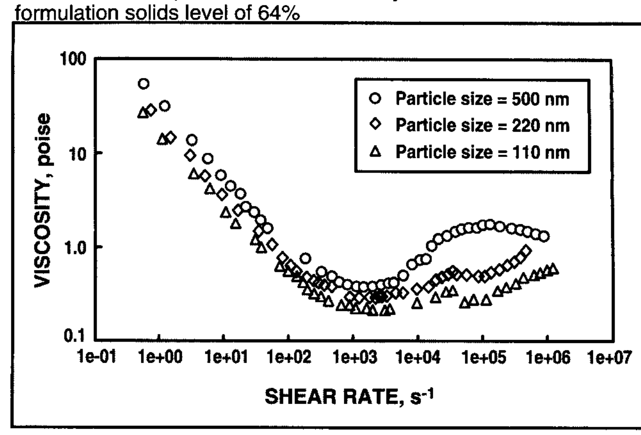

9. Effect of formulation solids level on viscosity versus shear rate data for latex particle size of 500 nm

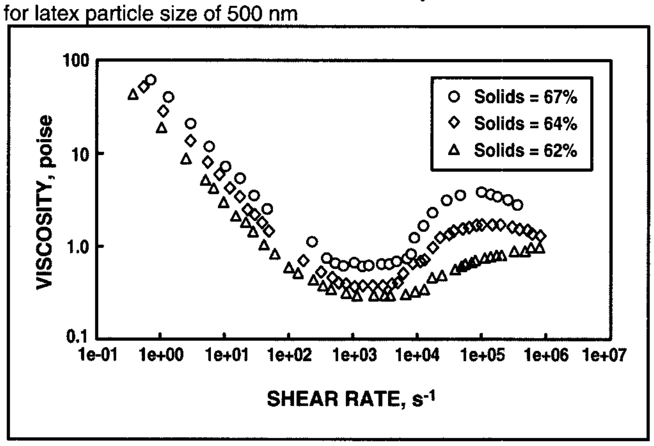

10. Effect of formulation solids level on viscosity versus shear rate data for latex particle size of 110 nm

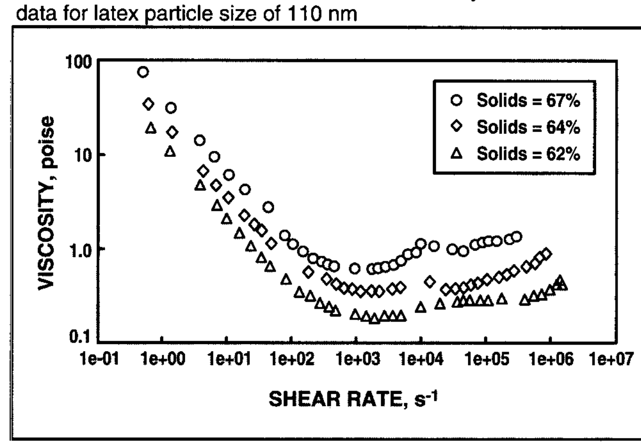

puter modeling to try to predict high-speed runnability.

Rheology data

During the coating process, the coating formulation experiences a wide range of shear rates within the short-dwell coater chamber. Thus, for modeling purposes, it is necessary to measure the flow properties of a formulation over the shear rate range from 0 to >1,000,000 s^{-1}. No single rheometer is able to span this entire shear rate range so data from several rheometers were combined. Rotational rheometers were used to collect the low- and intermediate-shear data, and a capillary rheometer was used to collect the high-shear data. Specifically, the Brookfield rheometer was used to measure the low-shear range (0.5–75 s^{-1}); the Haake Rotovisco rheometer with the MV SP bob and cup was used for the intermediate-shear range (100–5000 s^{-1}); the Hercules rheometer with the E bob and cup was used for the high-shear range (5000–45,000 s^{-1}); the Anton Paar HV6 capillary rheometer was used for the ultra-high-shear range (100,000–1,000,000 s^{-1}). The data from the capillary viscometer have been corrected for end effects, wall slip, and non-Newtonian flow (Rabinowitch correction).

Figure 5 shows how the data from the different rheometers can be combined to generate a single flow curve from 1 s^{-1} to 1,000,000 s^{-1}. This viscosity versus shear rate curve is typical for most starch-containing formulations. There is a power-law shear thinning region which levels off to a constant viscosity at high shear rates (>5000 s^{-1}). Actually this leveling off to a constant viscosity is only an approximation. If the high-shear data are plotted using a linear scale, the viscosity continues to decrease slightly. **Figure 6** shows other examples of starch-containing formulations where the latex particle size has been varied. The limiting high-shear viscosity increases as the latex particle size increases, and the shear-thinning behavior at ultra-high-shear becomes more pronounced.

There are other formulations which exhibit more complex viscosity versus shear rate behavior. An example of shear-thickening or dilatancy is shown in **Fig. 7**. There is a sharp rise in viscosity as shear rate increases followed by a slight decrease in viscosity at still higher shear rates. We are not sure if the observed decrease in viscosity at very high shear rates (1,000,000) is real or an artifact of the capillary viscosity measurement. In our pilot coater studies, we once used a blend of 75%

11. Flow curve for Cross model

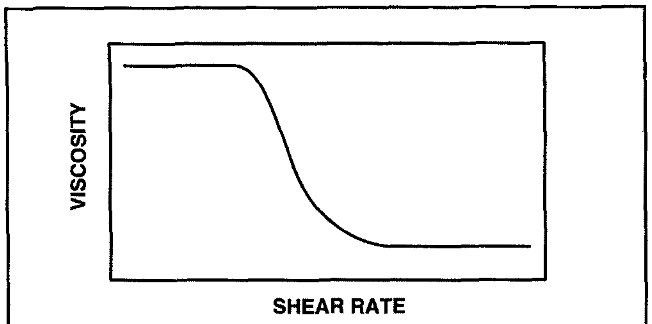

$$\frac{\eta - \eta_\infty}{\eta - \eta_\infty} = \frac{1}{(1 + k\dot{\gamma}^n)} \Rightarrow \eta - \eta_\infty + \frac{\eta - \eta_\infty}{(1 + k\dot{\gamma}^n)} = \eta_\infty + \frac{1000}{(1 + k\dot{\gamma}^n)}$$

12. Flow curve for Gillespie model

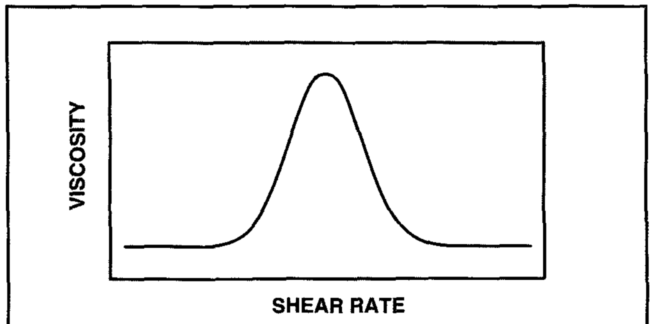

$$\eta = \eta_\infty + \frac{4Ea_c\,(\pi C_1 D + 4/3\, a_c^2 \dot{\gamma})\phi^2}{Vo^2\,(1/C_s\, t_B + \dot{\gamma})^2} \Rightarrow \eta = \eta_\infty + \frac{(k_2\dot{\gamma})}{(k_3 + \dot{\gamma})^2}$$

13. Combined model curves fitted to viscosity versus shear rate data for 500-nm latex

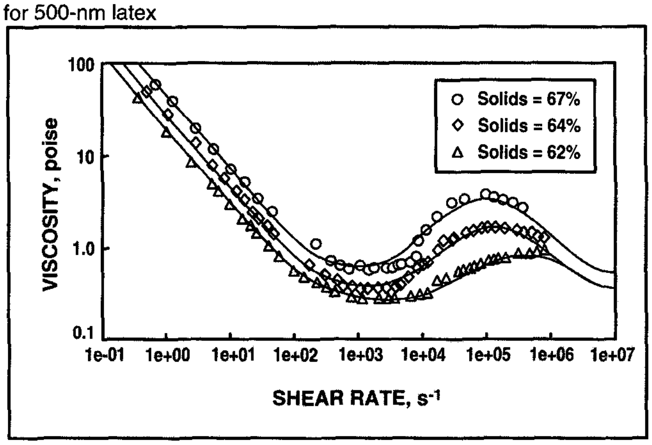

14. Combined model curves fitted to viscosity versus shear rate data for 110-nm latex

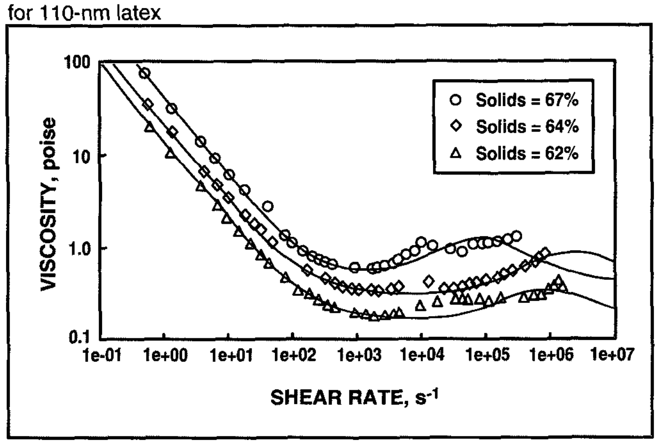

large-particle-size latex with 25% small-particle-size latex. This formulation had a viscosity versus shear rate curve similar to that in Fig. 7. This formulation exhibited severe blade weeping and poor coat weight profile, which improved as the coating speed increased. This suggests that the decrease in viscosity at higher shear rates seen in Fig. 7 is a real phenomenon.

There are several factors which impact the dilatant behavior of paper coatings. One key parameter is the latex particle size. **Figure 8** shows that at the same solids, decreasing latex particle size leads to less dilatancy and an increase in the shear rate where the viscosity begins to rise. **Figure 9** shows the impact of solids level. Not surprisingly, increasing solids leads to greater dilatant behavior and a slight shift to lower shear rates where the increase in viscosity begins. **Figure 10** shows that for a small particle size latex, there is a general increase in high-shear viscosity with increasing solids, but the dilatant behavior is greatly reduced.

Rheology model

In order to use the measured viscosity versus shear rate data in the CFD simulation, it was necessary to fit the data with a mathematical function. There are several rheological models which can be used to fit the data. A combination of a power-law fluid with a limiting high-shear viscosity fits the data for starch containing formulations very well. However, the power-law model leads to infinite viscosities at low shear rates, which causes computational problems. By contrast, the Cross model *(7)* shown in **Fig. 11** combines a power-law region with limiting low- and high-shear viscosities. However, measurements on coating formulations down to 0.001 s^{-1} using a constant stress rheometer showed that they did not approach a limiting low-shear viscosity. Instead, the formulations exhibited a yield stress. Although using rheology models incorporating a yield stress might seem better, these models also lead to computational problems because it is difficult to keep track of domains where the fluid is flowing and those where it is not. Therefore, for our rheology model, we used the Cross equation where we arbitrarily fixed the limiting low-shear viscosity to 1000 poise. This gives a three-parameter model which fits the available data and avoids the problems of the power-law model at very low shear rates.

15. Comparison of PHOENICS results for coarse grid simulation of flow in short-dwell chambers

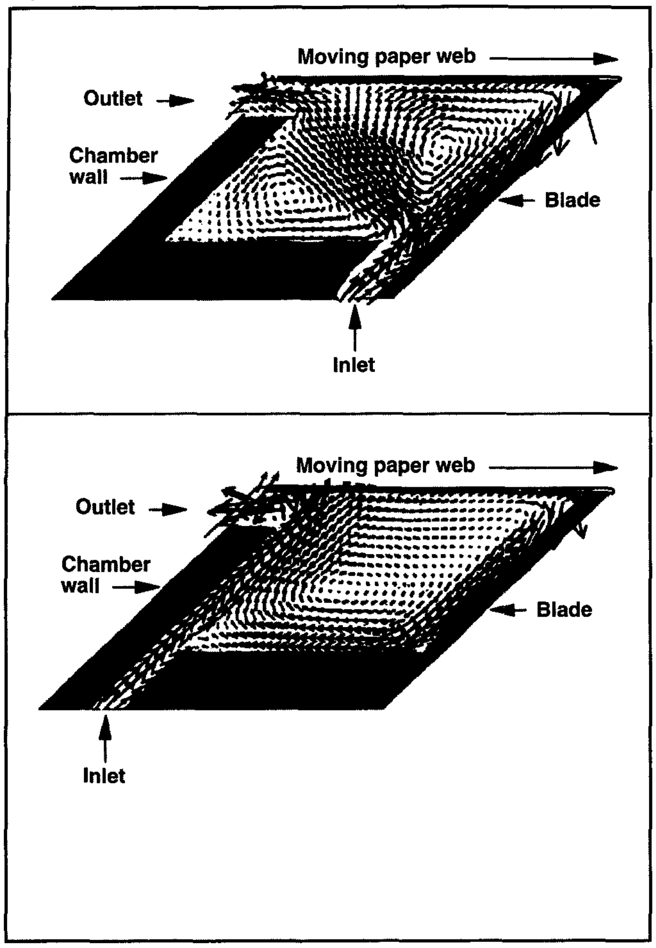

16. Comparison of velocity profiles next to paper web for Newtonian and shear-thinning (Cross) fluids

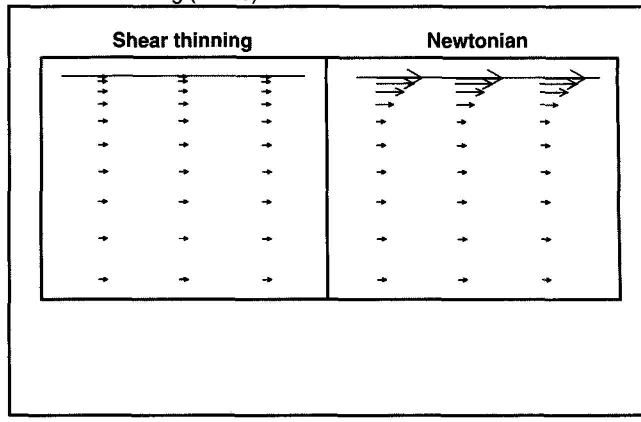

17. Comparison of calculated blade pressures for control formulation versus experimental values obtained at the pilot coater

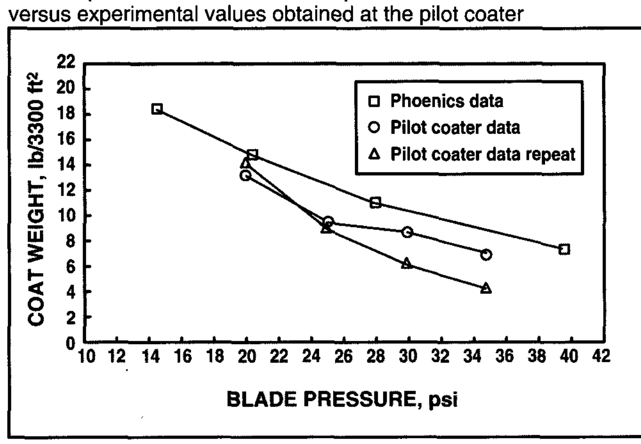

The Cross model has to be modified to fit the viscosity versus shear rate data shown in Figs. 7–10. There are several equations which have been used to describe dilatant behavior. Nearly all of these equations have only a shear-thickening transition and do not include subsequent shear-thinning behavior at still higher shear rates. One model which does give increasing and then decreasing viscosity at high shear rates is the Gillespie model *(8)* shown in **Fig. 12.** The Gillespie model is based upon the impulse theory where shear-induced structure building is caused by binary collisions between particles. This buildup of structure is followed by a breakdown of structure at still higher shear rates. The underlying basis for the Gillespie model is very similar to that for the Cross model. In the Cross model, there are flocculated aggregates between particles at low shear which are broken up as the shear rate is increased. Thus it seemed natural to combine the two models to fit the observed viscosity versus shear rate data for our formulations. The combined model can be written as:

$$\mu = 1000/(1+k_1\dot{\gamma}^n)+\mu_\infty+k_2\dot{\gamma}/(k_3+\dot{\gamma})^2 \quad (1)$$

There are five adjustable parameters in the model: k_1 and n describe the power-law shear thinning region, μ_∞ is the limiting high-shear viscosity, k_2 controls the magnitude of dilatancy, and k_3 is the critical shear rate for the onset of dilatant behavior. The fits of the model to the data are shown in **Figs. 13 and 14.** The combined model fits the data for the 500 nm latex very well. The model did a reasonable job in fitting the data for the 110 nm latexes, especially the high-shear data needed for modeling high-speed runnability. The parameters used in fitting the data are given in **Table I.**

CFD modeling

The second part of the modeling effort was the development of a simulation of the coating process using computational fluid dynamics (CFD). There has been a great deal of activity in recent years to model the flow in paper coaters *(9–12)*. Our objective was not to develop new CFD models but to use commercially available programs coupled with lab measurements and pilot coater data to achieve a more realistic simulation of the coating process. Eventually it is hoped to use CFD to understand the coating process and predict runnability without having to use a pilot coater. Our model is still in the early stages of development so only preliminary results are reported here.

I. Summary of model parameters

Particle Size	Solids, %	k_1	n	μ_∞	k_2	k_3
500 nm	67	16.7	0.851	0.356	1,860,000	138,000
	64	26.6	0.868	0.276	1,060,000	172,000
	62	41.8	0.879	0.254	1,410,000	494,000
220 nm	67	25.4	0.881	0.266	1,770,000	290,000
	64	43.5	0.859	0.227	1,020,000	479,000
	62	54.6	0.856	0.184	3,700,000	2,150,000
110 nm	67	22.3	0.892	0.465	280,000	80,700
	64	44.8	0.885	0.323	7,360,000	2,600,000
	62	73.5	0.861	0.162	1,010,000	1,030,000

The simulations presented here used PHOENICS, a commercial finite volume CFD code from CHAM UK. To date, only two-dimensional simulations of short-dwell coaters have been carried out. **Figure 15** shows the flow field calculated by PHOENICS using a coarse grid for two short-dwell coater geometries which differ in the location of the inlet. The flow in the chamber with the inlet next to the blade has much larger velocities and a vortex nearer the blade nip compared to the other geometry. The general features of these flow fields are in agreement with previously reported results *(9)* and flow visualization of short-dwell chambers by Eklund *(1)*.

For the coarse grid, there was not much qualitative difference in the flow field between using a Newtonian fluid and the shear-thinning Cross model. A calculation using a finer grid showed that most of the differences between the fluids occurred along the chamber walls and the moving paper web where the shear forces are greatest. **Figure 16** shows an expanded view of the flow field near the paper web. The shear-thinning Cross model fluid shows a more uniform velocity profile having lower average velocity than that for the Newtonian fluid. This difference will have a greater impact on flow in the blade nip than on the overall flow in the chamber.

In the blade nip, most of the hydrodynamic pressure due to the coating flow is concentrated at the tip of the blade. If one assumes that the blade is a perfectly stiff cantilevered beam with all of the hydrodynamic pressure applied to the tip and a restoring force applied to the blade 1/3 distance from the tip, then it is possible to calculate the blade pressure to achieve a given coat weight. In **Fig. 17**, the calculated blade pressures for the formulation having the flow curve shown in Fig. 5 are compared to actual pilot coater data. The calculated results are higher than the observed data. However, it is encouraging to see at this early stage of development the relatively good agreement between the simulation and pilot coater results. Future work will incorporate basestock compressibility, flexing of the blade, dewatering of the formulation, and a free surface at the blade nip exit. These more realistic modeling conditions should give better agreement between the pilot coater and predicted results.

Summary and conclusions

1. High-shear rheology is one of the key parameters controlling high-speed runnability. If operating conditions at the pilot coater were chosen to run on the land of the blade and minimize blade wear, then there was a good correlation between high-shear viscosity measured on a capillary viscometer and the blade pressure needed to achieve a target coat weight.
2. The viscosity of paper coating formulations has been measured from very low to very high shear rates using a combination of rheometers. The resulting viscosity versus shear rate curve can be fitted with a five-parameter model which includes dilatant behavior.
3. The flow in short-dwell coating chambers was simulated using the PHOENICS program and the results compared with pilot coater data. This CFD simulation included the rheology model developed to describe the flow curves of coating formulations.
4. Runnability is a complex phenomenon which is difficult to predict. By combining laboratory measurements with computer simulations, a better understanding of runnability can be achieved. TJ

Literature cited

1. Eklund D. E. and Norrdahl, P. C., TAPPI 1986 Coating Conference Proceedings, TAPPI PRESS, Atlanta, p. 99.
2. Gane P.A.C. and Coggon, L., Tappi J. 70(12): 87(1987).
3. Saito T. A. and Scriven, L. E., TAPPI 1985 Coating Conference Proceedings, TAPPI PRESS, Atlanta, p. 13.
4. Pranckh F. R. and Scriven, L. E., TAPPI 1988 Coating Conference Proceedings, TAPPI PRESS, Atlanta, p. 217.
5. Ortman B. J. and Donigian, D. W., TAPPI 1992 Coating Conference Proceedings, TAPPI PRESS, Atlanta, p. 217.
6. Gane, P.A.C., Watters, P., and McGenity, P. M., TAPPI 1992 Coating Conference Proceedings, TAPPI PRESS, Atlanta, p. 117.
7. Cross, M. M., J. Colloid Sci. 20: 417(1965).
8. Gillespie, T. J., J. Colloid Sci. 22: 554(1966).
9. Triantafillipoulos, N. G., Rudemiller, R., Farrington, T., *et al.*, TAPPI 1988 Coating Conference Proceedings, TAPPI PRESS, Atlanta, p. 47.
10. Aidun C. K. and Triantafillipoulos, N. G., TAPPI 1990 Coating Conference Proceedings, TAPPI PRESS, Atlanta, p. 309.
11. Affes, H., Conlisk, A, T., and Foster, M. R., TAPPI 1990 Coating Conference Proceedings, TAPPI PRESS, Atlanta, p. 299.
12. Conlisk, A. T. and Foster, M. R., TAPPI 1991 Coating Conference Proceedings, TAPPI PRESS, Atlanta, p. 327.

The authors thank Jim Beer, Dan Chase, Mark Pollock, Dave Wolf, and members of the Dow pilot coater staff for their assistance in collecting the data needed for the modeling work.

Received for review Dec. 9, 1992.

Accepted Dec. 17, 1992.

Presented at the TAPPI 1993 Coating Conference.

Pfizer Specialty Minerals Inc.

We've sharpened our future...we're now

Minerals Technologies Inc.

Who We Are
Everything you liked about Pfizer Specialty Minerals for over 30 years is the same. The people, the products, the services and commitment. What's changed is our name and our potential. So if you've done business with **Specialty Minerals** or **Quigley**, you'll now be working with Minerals Technologies Inc. And if you've never done business with us, here's a look at our capabilities.

What We Are
MTI is the leading producer and supplier of precipitated calcium carbonate (PCC) — an economical filler substitute for costly wood fiber, also used in plastics, sealants and paints. We have more than 30 PCC plants, with plans to expand worldwide.

We're one of the world's leading developers of minerals-based refractory materials used by the steel, cement and glass industries.

We mine and process limestone and talc and manufacture calcium metal, lime, and metallurgical cord wires. Limestone and talc are used in building materials, paints and coatings, plastics, and ceramics. Calcium metal's primary use is the production of batteries and magnets, while cord wire is used in iron, steel and non-ferrous metal production.

Where We Are Going
Our commitment to research and development continues. New product development is a major goal. MTI already has over 250 worldwide patents and 340 trademarks and is committed to maintaining industry leadership in research and development.

Our recently patented acid-tolerant PCC technology will broaden our involvement in papermaking. In plastics we are introducing ultrafine talc and we continue to pioneer new PCC products for sealant applications as well.

In the refractory product area, we are developing products that will aid a variety of furnaces and other high temperature vessels that are difficult to line with refractory bricks.

A Commitment To Your Future
MTI's crystal engineering abilities can create new morphologies to support papermakers who want to replace fiber with filler, improve optical quality of their products and stay on the forefronts of alkaline papermaking. This technology, coupled with our ability to offer fine ground natural products, positions MTI to support your long-term product development efforts in other industrial applications as well. Our commitment to quality encompasses every single aspect of our organization from product development through customer service. This dedication to our future and yours is substantial. Join us and share in it. For more information, call (215) 882-8700 or write: Marketing Director, Minerals Technologies Inc., 35 Highland Avenue, Bethlehem, PA 18017.

MINERALS TECHNOLOGIES

SPECIALTY MINERALS INC. ...BARRETTS MINERALS INC. ...MINTEQ INTERNATIONAL INC.

Circle No. 446 on Reader Service Card **We're more than just minerals**